International Journal of Nanomedicine

Dovepress
open access to scientific and medical research

Open Access Full Text Article

ORIGINAL RESEARCH

Proliferation and stemness preservation of human adipose-derived stem cells by surface-modified in situ TiO_2 nanofibrous surfaces

This article was published in the following Dove Press journal:
International Journal of Nanomedicine
21 November 2014
Number of times this article has been viewed

Ai Wen Tan[1]
Lelia Tay[2]
Kien Hui Chua[2]
Roslina Ahmad[3]
Sheikh Ali Akbar[4]
Belinda Pingguan-Murphy[1]

[1]Department of Biomedical Engineering, University of Malaya, Kuala Lumpur, Malaysia; [2]Department of Physiology, Faculty of Medicine, National University of Malaysia, Kuala Lumpur, Malaysia; [3]Department of Mechanical Engineering, University of Malaya, Kuala Lumpur, Malaysia; [4]Department of Materials Science and Engineering, The Ohio State University, Columbus, OH, USA

Abstract: Two important criteria of an ideal biomaterial in the field of stem cells research are to regulate the cell proliferation without the loss of its pluripotency and to direct the differentiation into a specific cell lineage when desired. The present study describes the influence of TiO_2 nanofibrous surface structures on the regulation of proliferation and stemness preservation of adipose-derived stem cells (ADSCs). TiO_2 nanofiber arrays were produced in situ onto Ti-6Al-4V substrate via a thermal oxidation process and the successful fabrication of these nanostructures was confirmed by field emission scanning electron microscopy (FESEM), energy dispersive spectrometer (EDS), X-ray diffractometer (XRD), and contact angle measurement. ADSCs were seeded on two types of Ti-6Al-4V surfaces (TiO_2 nanofibers and flat control), and their morphology, proliferation, and stemness expression were analyzed using FESEM, AlamarBlue assay, flow cytometry, and quantitative real-time polymerase chain reaction (qRT-PCR) after 2 weeks of incubation, respectively. The results show that ADSCs exhibit better adhesion and significantly enhanced proliferation on the TiO_2 nanofibrous surfaces compared to the flat control surfaces. The greater proliferation ability of TiO_2 nanofibrous surfaces was further confirmed by the results of cell cycle assay. More importantly, TiO_2 nanofibrous surfaces significantly upregulate the expressions of stemness markers Sox-2, Nanog3, Rex-1, and Nestin. These results demonstrate that TiO_2 nanofibrous surfaces can be used to enhance cell adhesion and proliferation while simultaneously maintaining the stemness of ADSCs, thereby representing a promising approach for their potential application in the field of bone tissue engineering as well as regenerative therapies.

Keywords: titania, nanofibers, thermal oxidation, stem cells, pluripotency

Introduction

Stem cells are unspecialized master cells characterized by self-renewal and pluripotential differentiation. They can be guided to become cells of a specific lineage under desirable cellular microenvironments.[1,2] Mesenchymal stem cells (MSCs) are a subpopulation of stem cells isolated from bone marrow that have the ability to self-differentiate into multiple mesenchymal lineages such as osteoblasts, chondrocytes, adipocytes, endothelial cells, fibroblasts, and myocytes.[3–6] Characterized by a high self-renewal rate, these cells are regarded as a potential candidate for bone tissue engineering,[3,7] as well as for use within in vitro models for tissue–biomaterial response testing.[8,9]

Recently, human adipose–derived stem cells (ADSCs) have aroused tremendous research interest as alternative sources of MSCs primarily because of their ease of isolation, extensive proliferation ability, and hypoimmunogenic nature.[10] Unlike MSCs, they represent an abundant source of pluripotent stem cells that can be easily isolated from subcutaneous adipose tissue through minimally invasive procedures such as

Correspondence: Belinda Pingguan-Murphy
Department of Biomedical Engineering, University of Malaya, Kuala Lumpur, Malaysia
Tel +603 7967 4491
Fax +603 7967 4579
Email bpingguan@um.edu.my

liposuction or resection.[11] They are reported to result in low donor site morbidity, have a high yield at harvest, and are more easily expandable in vitro than MSCs.[7,12] In addition, as with MSCs, they can also be guided into multiple lineages under a favorable microenvironment; these include osteogenic, adipogenic, chondrogenic, and myogenic lineages.[13,14] Taken together with all these advantages, the use of ADSCs as an alternative stem cell source for various biomedical applications holds great promise.

Stem cell studies have become a prominent research topic in the field of biomaterials. An ideal implant should possess two criteria: the first is to direct the differentiation of stem cells into the desired cell lineage; and the second is to allow the stem cells to trigger proliferation without losing their pluripotency or stemness.[15,16] Both criteria are reported to be closely related to the surface topography of the implants since the clinical success of any implant depends on the interaction between the surface of the implant and the surrounding tissue.[17] Indeed, it has been proven in recent studies that nanotopography is the main influencing factor, rather than the conventional microtopography.[18] A number of promising results with enhanced cellular behavior were reported on nanostructured surfaces as compared to the conventional microstructured surfaces.[18–20] While there is a growing body of evidence demonstrating the importance of substrate nanotopography in inducing directed stem cell differentiation using various inducing media or biological stimuli,[20–23] little attention has been paid to the impact of this factor in maintaining the stemness of stem cells. Dalby et al reported that stemness of MSCs is better retained when cells are cultured on ordered square nanostructures but not on flat substrates.[24] Zhang and Kilian also reported that stemness of MSCs was well-preserved with high expression of mesenchymal stemness markers when cells adhered to nanoisland patterned polydimethylsiloxane (PDMS) surfaces compared to nonpatterned surfaces.[3] Together, they showed that substrate nanotopography was the key to influencing stemness maintenance of stem cells. Clearly, further studies are needed to establish the role of surface topography in preserving the stemness of the stem cells and the current paper addresses that.

Titanium (Ti) and its alloys are well-known as biomaterials of interest for orthopedic applications, as they have been found to be highly corrosion resistant and biocompatible, as well as having favorable mechanical properties.[25,26] However, due to the inherent inertness of the protective TiO_2 layer that forms on their surfaces when exposed to the atmosphere, their widespread acceptance for orthopedic implants has been limited.[22] A simple solution has been suggested, that is to modify their surface topography while maintaining the mechanical advantages of a Ti-based implant.[27] Various morphologies of TiO_2 have been introduced onto the surfaces of Ti-based substrates, including nanotubes, nanofibers (NFs), and nanorods and they can be fabricated by various techniques such as electrospinning, anodization, and hydrothermal treatment.[28] However, some of these methods give rise to several concerns such as the problems of phase purity, crystallinity, and incorporation of impurity.[29] For example, the crystallinity of TiO_2 nanostructures prepared by electrospinning and anodization is usually not satisfactory and thus additional heat treatment is needed to improve the crystallinity of TiO_2 nanostructures.

Our group has recently introduced TiO_2 NFs on Ti6-Al-4V substrate surface by using a thermal oxidation process under limited oxygen (O) supply with a controlled flow rate, which has been proven to be an effective substrate for significantly enhanced cellular behavior.[28,30,31] Our own studies with human osteosarcoma (HOS)-derived cell line on these nanofibrous surfaces revealed improved cell adhesion and cell proliferation on TiO_2 NF–coated substrate compared to the other counterparts.[31] Our more recent studies also showed that these nanofibrous surface structures are suitable for use as an effective substrate for cartilaginous applications.[28] In this study, the results indicated that TiO_2 nanofibrous substrate triggers enhanced chondrocyte adhesion, proliferation, and production of extracellular matrix (ECM) fibrils when compared to a flat control substrate.

To further confirm the clinical feasibility of such nanofibrous surface structures produced via thermal oxidation, the current study was designed to investigate the cellular interaction between these surface structures and stem cells, since stem cells are demonstrated to possess the capability of self-renewal and multi-lineage differentiation. In the present study, we tested the hypothesis that these TiO_2 nanofibrous surface structures can promote the proliferation of ADSCs without causing loss of their stemness by culturing them in a normal culture medium. Initial cell adhesion, cell proliferation, cell cycle progression, and gene expression of ADSC stemness markers were examined on the TiO_2 nanofibrous surface structure produced via the thermal oxidation method as compared to the bare Ti-6Al-4V substrates that were used as the control.

Materials and methods

Preparation and characterization of TiO_2 nanofiber arrays

In situ TiO_2 NFs were created on Ti-6Al-4V discs using a thermal oxidation process similar to the method described

previously.[28,31] To explain briefly, Ti-6Al-4V discs (grade #5, Titan Engineering Pte Ltd, Singapore) of size ø 6.35×2 mm were employed as test substrates. The discs were polished using silicon carbide (SiC) sandpaper of grit 1,200 prior to the oxidation treatment. After degreasing the discs in acetone, methanol, and distilled water sequentially, the discs were etched in a solution of HCl at 80°C for 10 minutes to remove any native oxide layer. The discs were then rinsed with water and left to air dry. The oxidation process was carried out in a horizontal tube furnace (Lindberg, TF55035C; Thomas Scientific, Swedesboro, NJ, USA). The substrate was located at the center of the furnace and a constant flow of 750 mL/minute Argon gas (99.999% purity) was introduced into the furnace as the carrier gas. The furnace temperature was maintained at 700°C and held for 8 hours before rapid quenching to room temperature. An identical size of polished Ti-6Al-4V disc was used as the control substrate after being degreased as described earlier. The morphology and composition analysis of the two samples was examined by field emission scanning electron microscope (FESEM; Zeiss Gemini; Carl Zeiss Meditec AG, Jena, Germany) equipped with an energy dispersive spectrometer (EDS; INCA; Oxford Instruments, Abingdon, UK). The crystallinity of the samples was studied by using an X-ray diffractometer (XRD, PANalytical Empryean, Almelo, the Netherlands) fitted with CuKα radiation (λ=0.154 nm) in the range of 2θ=20°–80°. The measurement of the contact angle for each surface was obtained by using a contact angle measurement system (model OCA 15 EC; Dataphysics Instruments, Filderstadt, Germany). The value of the contact angle was expressed as the mean ± standard deviation (SD) of three replicate measurements. All the discs were sterilized by autoclaving prior to cell seeding.

Isolation and cultivation of human adipose–derived stem cells

This research was conducted with ethical approval from the Universiti Kebangsaan Malaysia Research and Ethical Committee (Reference number: UKM 1.5.3.5/244/UKM-FF-FRGS0165-2010). Human ADSCs were isolated from the adipose tissue of patients who underwent cesarean section at Universiti Kebangsaan Malaysia Medical Centre with informed consent. The specimens were placed in sterile containers and brought to the Biotechnology Laboratory, Department of Physiology, Faculty of Medicine, Universiti Kebangsaan, Malaysia to be processed within 24 hours. Adipose tissue was minced into very fine pieces and digested in 0.3% Collagenase Type 1 Solution (Worthington Biochemical Corporation, Lakewood, NJ, US) for 45 minutes at 37°C. Digested tissue was centrifuged to harvest the cell pellet that was subsequently washed with phosphate-buffered saline (PBS). The isolated cells were cultured in Dulbecco's Modified Eagle Medium-Ham's F12 medium (DMEM: F12; 1:1; Thermo Fisher Scientific, Waltham, MA, USA) supplemented with 10% fetal bovine serum (FBS; Thermo Fisher Scientific), 1% antibiotic-antimycotic (Thermo Fisher Scientific), 1% glutamax (Thermo Fisher Scientific), and 1% vitamin C (Sigma-Aldrich Co., St Louis, MO, USA). The ADSCs were maintained at 37°C and 5% CO_2 with medium refreshed every 3 days. After reaching 70% confluence, the primary culture represented as passage 0 (P0) was trypsinized using 0.125% trypsin–EDTA (Thermo Fisher Scientific) and passaged at a culture expansion ratio of one to four until passage five (P5).

Cell adhesion

ADSCs were seeded on the samples at a density of 5×10^4 cells/cm^2 and cultured for 1, 3, 7, and 14 days, with medium refreshed every 2 days. Morphological analysis of ADSCs cultured on both the samples (TiO_2 NFs and flat control) was observed using FESEM. Briefly, after the prescribed time points, the samples were washed thrice with PBS and fixed with 2.5% formalin solution (Sigma-Aldrich Co.) for 1 hour. The samples were rinsed thrice again with PBS after fixation and dehydrated using a gradient of ethanol concentration. After drying overnight in a freeze dryer (FreeZone; Labconco, Kansas City, MO, USA), the samples were eventually observed by FESEM.

Cell proliferation assay

Cell viability of ADSCs on both the samples was assessed by AlamarBlue assay (Thermo Fisher Scientific) according to the manufacturer's protocol. Briefly, ADSCs were cultured on the sample surface for 1, 3, 7, and 14 days. After predefined incubation times, the samples were washed with PBS three times to remove nonadherent cells. To check for cell viability, cells were incubated with 10% AlamarBlue in complete media for 4 hours and the optical density (OD) was measured using a microplate reader at 570 nm, with 600 nm set as the reference wavelength. The cell number was determined from a standard graph generated for different seeding densities of ADSCs on 24-well plates and the OD was evaluated the same way using the AlamarBlue assay.

Cell cycle progression analysis

ADSCs cultured on both the samples were harvested at day 14 after trypsinization and were rinsed three times with

buffer solution with adjusted concentration, 5×10^5 cells/mL, and prepared using CycleTEST PLUS DNA Reagent Kit (BD Biosciences, San Jose, CA, USA) according to the manufacturer's instructions. ADSCs were centrifuged at 1,000 rpm and the supernatant was discarded. Cells were resuspended with trypsin in a spermine tetrahydrochloride detergent buffer. After incubation, cells were suspended with trypsin inhibitor and ribonuclease A in citrate stabilizing buffer and transferred to a sterile flow cytometer glass tube. Then, 200 μL of propidium iodide (PI) was added, and incubation was done in the dark on ice.

Cell cycle status was analyzed by flow cytometer using PI as a specific fluorescent dye probe. The PI fluorescence intensity of 2.5×10^5 cells was measured for each sample using a FACS Calibur Flow Cytometer (BD Biosciences). The percentage of ADSCs in G0/G1, S, and G2/M phases were determined by Mod Fit software for cell cycle distribution. Cell cycle distribution was analyzed using CellQuest™ software (BD Biosciences) in the flow cytometry (FACS Canto II; BD Biosciences). The DNA histograms for each sample were determined using BD FASCS Diva software.

Total RNA extraction and gene expression analysis by quantitative real-time polymerase chain reaction

Total RNA were isolated from the ADSC cells cultured on control surfaces and TiO_2 nanofibrous surfaces using TRI reagent (Molecular Research Center, Inc., Cincinnati, OH, USA) by referring to the manufacturer's protocol. Polyacryl carrier (Molecular Research Center, Inc.) was added to precipitate the total RNA and the extracted RNA pellet was then washed with 75% ethanol and dried before dissolving it in RNase and DNase free distilled water (Thermo Fisher Scientific). The extracted RNA was immediately stored at −80°C until further analysis. Complementary DNA was synthesized from 100 ng of total RNA with SuperScript III reverse transcriptase (Thermo Fisher Scientific) according to the protocol recommended by the manufacturer. The protocol conditions were 10 minutes at 23°C for primer annealing, 60 minutes at 50°C for reverse transcription, and 5 minutes at 85°C for reaction termination. The cDNA was stored at −20°C until further analysis.

Quantitative PCR analysis was used to quantify the expression level of pluripotency-associated transcription factors and cell cycle–regulated genes, including Sox-2, Rex-1, Nanog3, Nestin, CyclinD1, pRb, GADD45, and p53. The expressions of all these genes were evaluated by a two-step reverse transcriptase–polymerase chain reaction (Thermo Fisher Scientific). Expression of glycerylaldehyde-3-phosphate dehydrogenase (GAPDH) gene was used as an internal control to ensure specificity of reaction. The primers (sense and antisense) used in the reaction were designed from the NIH Genebank database as shown in Table 1. The two-step real-time polymerase chain reaction (RT-PCR) reaction was performed using SYBR Green as the indicator in a Bio-Rad iCycler (Bio-Rad Laboratories Inc., Hercules, CA, USA). Each reaction mixture consisted of SYBR Select Master Mix (Thermo Fisher Scientific, Waltham, MA, USA), forward and reverse primers (5 μM each), deionized water, and 2 μL of cDNA template. The reaction conditions were: cycle 1: 95°C for 2 minutes (1×) and cycle 2: step 1 95°C for 10 seconds and step 2 56°C for 20 seconds (50×), followed by melting curve analysis. The results are given as a relative gene expression normalized to GADPH gene and is calculated using the formula: $2^{\text{Ct value of GADPH} - \text{Ct value of target gene}}$ where Ct is the value of cycle threshold fluorescence.

Statistical analysis

All the data were tested for statistical significance using SPSS software (v19; IBM Corporation, Armonk, NY, USA). Each experiment was performed in triplicate unless stated otherwise. Values were presented as mean ± standard error of mean (SEM) and the difference between groups was analyzed using Student's *t*-test and one-way analysis of variance (ANOVA). A *P*-value of less than 0.05 was considered significant.

Results

Surface analysis of TiO_2 nanofiber arrays

Figure 1 presents FESEM images of the control Ti-6Al-4V and as-grown TiO_2 nanofibrous surfaces. As depicted in the images, the surfaces of the control Ti-6Al-4V were relatively smooth, although some pits and irregular grinding marks were observed (Figure 1A), which were presumably incurred by the impact of the sandblasted particles during mechanical polishing. After 8 hours of thermal oxidation, a relatively high density of nanofiber arrays was observed to have formed homogeneously on the entire surface of the Ti-6Al-4V substrate (Figure 1B), which ranged in size from about 50 nm in diameter and about 785 nm in length. The respective water contact angles of each surface are displayed in the upper right corner of the FESEM images in Figure 1, showing that TiO_2 nanofibrous surfaces induced a significant increase in surface wettability, with the contact angle decreasing from 56.5°±2.2° on the control surfaces to 6.76°±0.86° on the nanofibrous surfaces.

Table 1 Description of primers used in RT-PCR for gene expression analyses

Gene	Accession no	Primers 5′ → 3′	PCR product (bp)
GAPDH	NM_001082253.1	F: caa cga att tgg cta cag ca R: aaa ctg tga aga ggg gca ga	186
Sox-2	NM_003106	F: ttacctcttcct ccc act cca R: ggtagtgctgggacatgtgaa	132
Rex-1	NM_174900	F: aaaggttttcgaagcaagctc R: ctgcgagctgtt tag gat ctg	185
Nanog3	NM_024865	F: ctgtgatttgtgggcctgaa R: tgtttgcctttgggactggt	153
Nestin	NM_006617	F: tccaggaacggaaaatcaag R: gcctcctcatcccct act tc	120
P53	NM_001126112.2	F: ccc agc caa aga aga aac ca R: gtt cca agg cct cat tca gct	101
pRB	NM_000321	F: cag acc cag aag cca ttg aa R: ctg ggt gct cag aca gaa gg	115
GADD45	NM_052850	F: cca aga tgc cac aga tga ttg R: act cct tgg gtc cac ctg gta	140
CyclinD1	NM_053056	F: aga cct tcg ttg ccc tct gt R: cag tcc ggg tca cac ttg at	181

Abbreviations: bp, base pairs; PCR, polymerase chain reaction; RT-PCR, real-time polymerase chain reaction.

Changes in the elemental composition and phase content were revealed by the EDS and XRD analyses as shown in Figure 2. The EDS analysis of the samples before and after the thermal oxidation process confirmed the presence of TiO_2 on the nanofibrous surfaces. Around 30.41%±0.10% (atomic concentration) of Ti and 66.81%±0.13% (atomic concentration) of O were observed on the nanofibrous surfaces, which correspond to a Ti to O atomic ratio of 2:1, same as the TiO_2 stoichiometry. The results again confirmed that as-grown NFs are mainly composed of TiO_2 after the oxidation process. XRD analysis of the nanofibrous surfaces produced by the thermal oxidation process yielded major diffraction peaks for crystalline oxide of Ti. The diffraction peaks located at 27.5, 36.1, and 54.3 were attributed to the (110), (101), and (111) planes of TiO_2 phase, respectively, which were well-indexed to the rutile TiO_2 phase with lattice constants of a=4.593 Å, c=2.959 Å, and the space group of P42/mnm (no. 136) (JCPDS file No. 21-1276). The results once again confirm that crystalline TiO_2 NFs were successfully fabricated using the thermal oxidation technique. Moreover, the average nanofiber size was estimated using the Scherrer equation[32] from the diffraction peaks in Figure 2. The average nanofiber size as calculated from the equation is 52.43 nm, which is close to the average nanofiber size estimated from the FESEM images.

Cell morphology and adhesion assessment

The morphology and spreading of ADSCs upon contact with the TiO_2 nanofibrous surfaces were examined using FESEM.

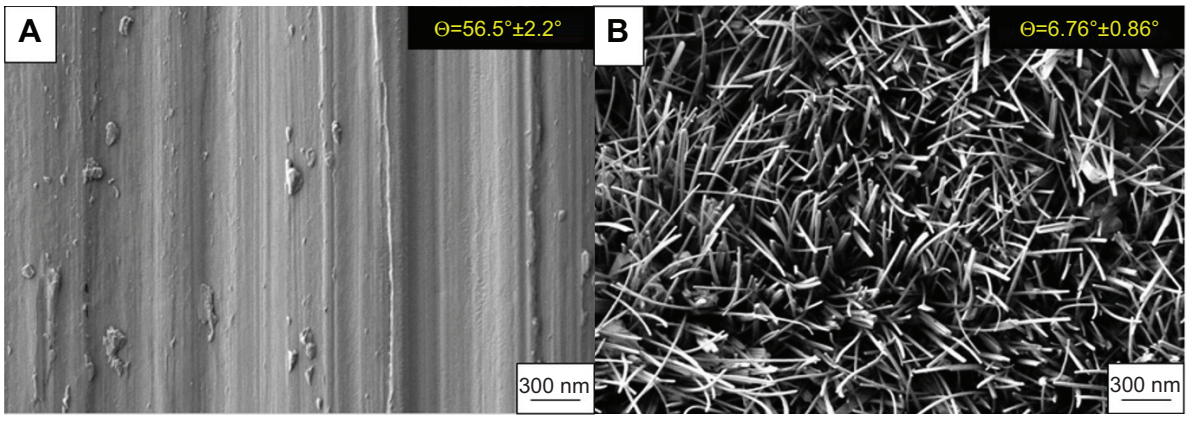

Figure 1 FESEM images of the (**A**) control Ti-6Al-4V substrate and the (**B**) fabricated TiO_2 nanofiber arrays.
Note: The upper right insets show the respective water contact angle of each surface.
Abbreviation: FESEM, field emission scanning electron microscopy.

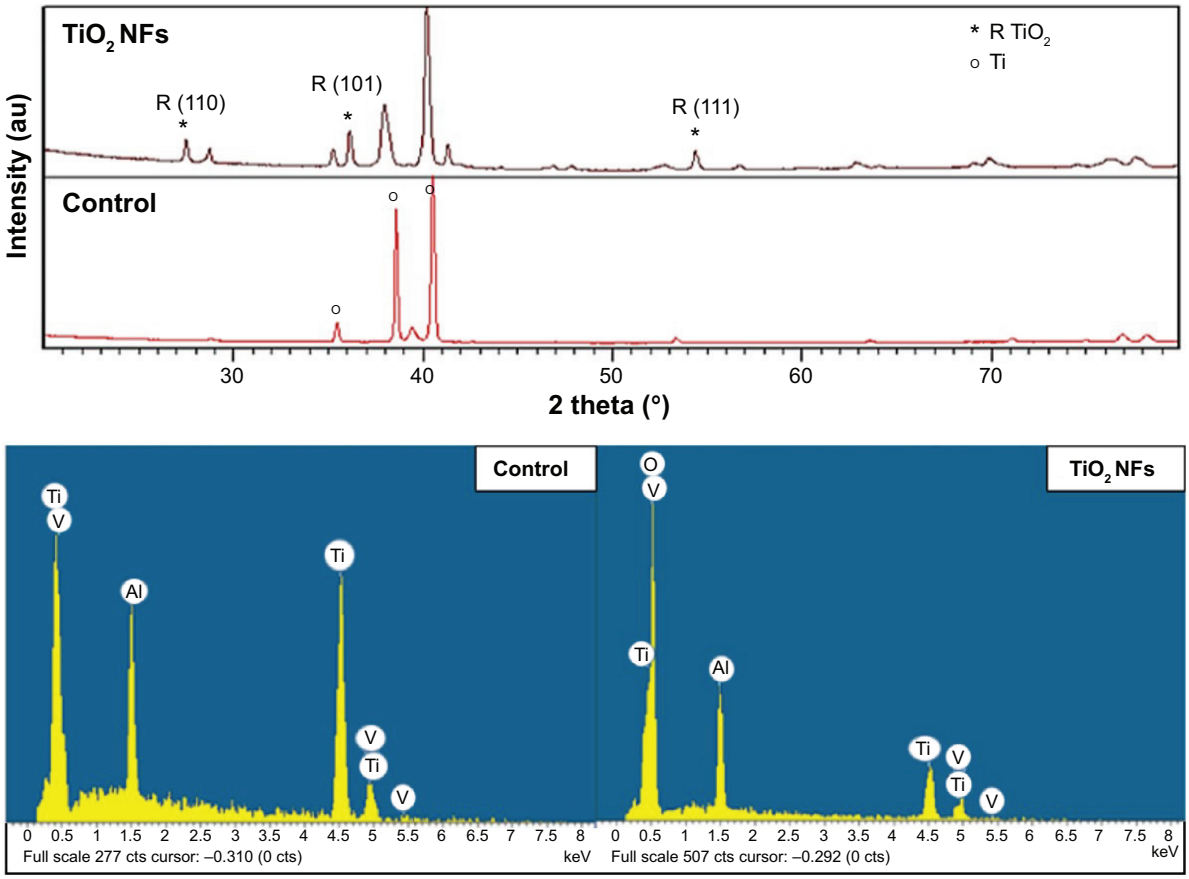

Figure 2 Respective XRD pattern and EDS spectrum of the flat control sample and the as-grown TiO_2 nanofiber arrays.
Abbreviations: EDS, energy dispersive spectrometer; NFs, nanofibers; R, rutile; XRD, X-ray diffractometer.

Figure 3 shows the FESEM images of adhered ADSC morphologies on nanofibrous structure, compared to control polished Ti-6Al-4V after 2 weeks of cell incubation. These images give visual evidence that adhered ADSCs presented a polygonal morphology and displayed good spreading, with greater spreading areas of the cells on the nanofibrous surfaces in comparison to their control counterparts, especially after 7 and 14 days of culturing. On day 14, noticeable filopodia and lamellipodia were projected out from the cells to anchor onto the nanofibrous surfaces and formed an intercellular connection with the adjacent cells, which is a good sign of cell-to-cell communication. On the contrary, the adhered ADSCs only displayed smooth spreading on the featureless control surface. This is because the flat Ti-6Al-4V substrate contains lesser topological cues and thus does not provide sufficient attachment for the cells to anchor to.

Cell proliferation

The AlamarBlue assay was used to investigate the proliferation of ADSCs cultured on the control and TiO_2 nanofibrous surfaces. This assay is based on a mechanism that blue resazurin can only be reduced to red resorufin by proliferating cells. Therefore, the production of resorufin indirectly reflects cell proliferation. Figure 4 shows the number of healthy ADSCs adhered to both the surfaces after being cultured for 1, 3, 7, and 14 days. As depicted in Figure 4, healthy ADSCs grown on the nanofibrous surfaces exhibited significantly higher cell proliferation than those cultured on the control surfaces over the incubation period ($P<0.05$), especially on day 14, indicating significantly enhanced cell growth.

Cell cycle analysis

Analysis of DNA content and the cell distribution at various phases of cell cycle (G0/G1, S, and G2/M) were performed using flow cytometer after 2 weeks of culturing and their results are shown in Figure 5 and Table 2, respectively. As revealed from the DNA histogram in Figure 5, no evidence that aneuploidy was found on either surface since there is only a single peak in the G0/G1 phase.[33] In the cell cycle, the primary phases that are responsible for cell proliferation are the S and G2/M phases,[34] and therefore the proliferation index (sum of the percentage of cells in S and G2/M phases) was

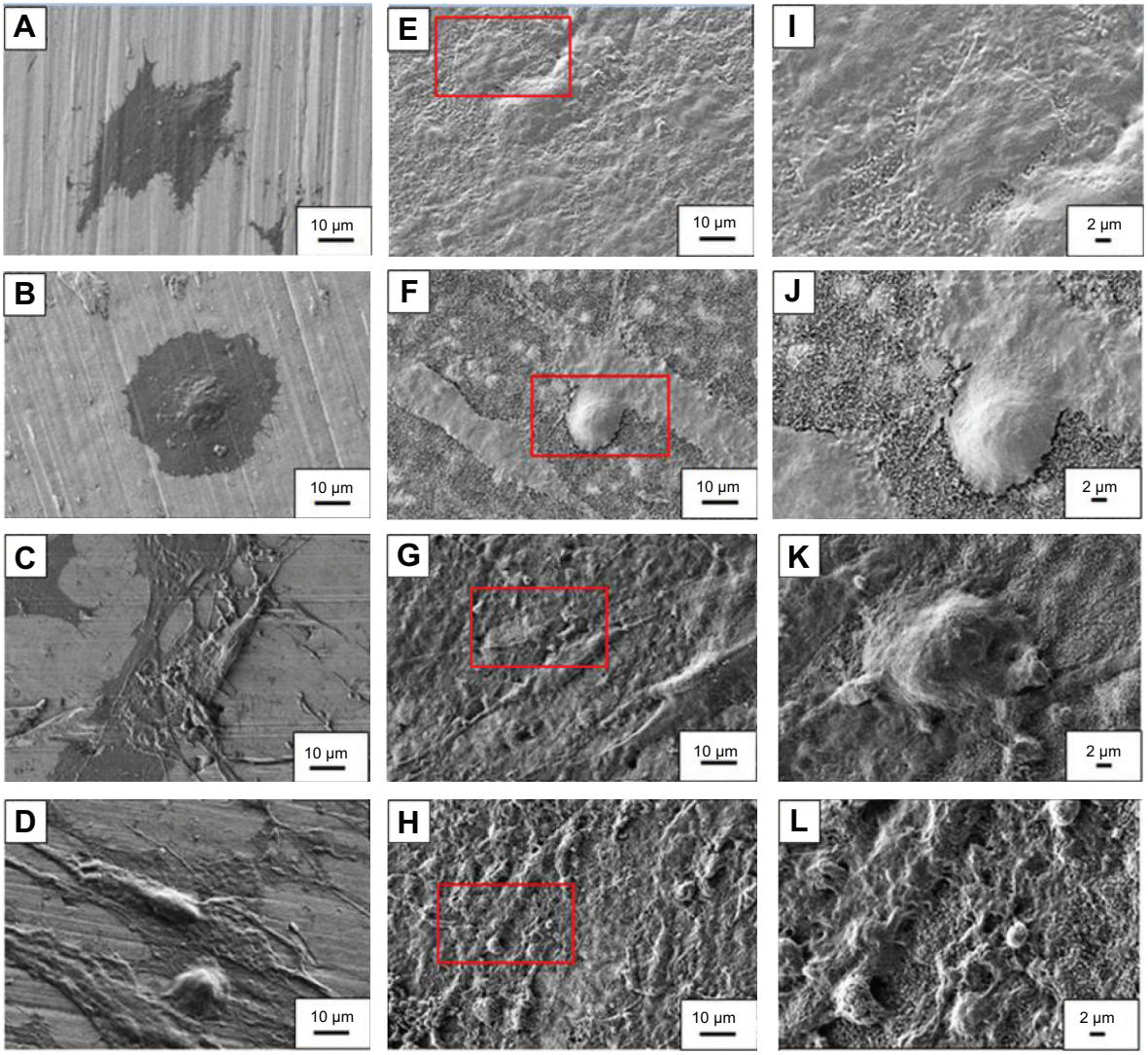

Figure 3 FESEM images show ADSCs adhered on control samples after (**A**) day 1, (**B**) day 3, (**C**) day 7, and (**D**) day 14 of culture compared to TiO_2 nanofibrous surfaces after (**E**) day 1, (**F**) day 3, (**G**) day 7, and (**H**) day 14 of culture.
Note: The area highlighted by the red box is shown in higher magnification in the images (**I**, **J**, **K**, and **L**) on days 1, 3, 7, and 14, respectively.
Abbreviations: ADSCs, adipose-derived stem cells; FESEM, field emission scanning electron microscopy.

calculated to assess the cell proliferation capacity of both surfaces (Table 2). In the G0/G1 phase, TiO_2 nanofibrous surfaces showed a significantly lower percentage of cells compared to the control surfaces. However, a significantly higher proliferation index was observed on the nanofibrous surfaces than their control counterparts ($P<0.05$). This result demonstrates that TiO_2 nanofibrous surfaces induce greater proliferation ability in ADSCs while maintaining the normal diploid state of the cells.

Gene expression of stemness markers and cell cycle control genes

To examine the degree of ADSC proliferation at the molecular level, the mRNA level of cell cycle–regulated genes, including CyclinD1, pRb, GADD45, and p53 were analyzed using real-time PCR after being cultured for 7 and 14 days; the results are shown in Figure 6. Quantitatively, compared to those cultured on the control surfaces, ADSCs grown on the nanofibrous surfaces displayed significantly higher expressions of all the cell cycle–regulated genes ($P<0.05$) at all time intervals.

We also examined the impact of substrate topography on retaining ADSC stemness, by analyzing the relative mRNA expression of pluripotency-associated transcription factors such as Nanog3, Rex-1, Sox-2, and Nestin quantitatively after 7 and 14 days of culturing on both the sample surfaces. Generally, our data in Figure 7 show that the expression levels of all the stemness markers for both the sample surfaces

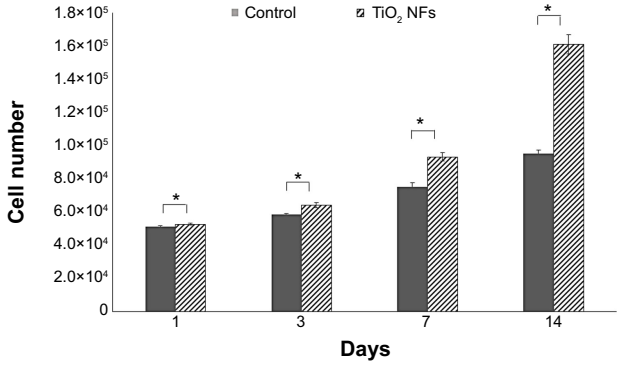

Figure 4 Cell proliferation of ADSCs cultured on TiO_2 nanofibrous surfaces in comparison to the flat control sample at days 1, 3, 7, and 14.
Note: Statistical significance was assessed relative to the control sample for each day (*$P<0.05$).
Abbreviations: ADSCs, adipose-derived stem cells; NFs, nanofibers.

were upregulated in a timely manner, from day 7 to day 14, with the gene expression level of ADSCs seeded on the nanofibrous surfaces being significantly higher than that of the control surfaces at each time point ($P<0.05$). In addition, the upregulation of all these stemness gene expression levels was found to be more robust on the TiO_2 nanofibrous surfaces than the control surfaces, from day 7 to day 14, indicating a greater ability of nanofibrous surfaces in preserving the stemness of ADSCs.

Discussion

In the present study, a simple oxidation-based surface modification technique, namely thermal oxidation, was used, which resulted in the growth of in situ TiO_2 NFs on Ti-6Al-4V substrates under a limited supply of oxygen and controlled flow rate. The fabrication of TiO_2 nanofibrous surface structures onto Ti-6Al-4V substrate was clearly revealed by FESEM observation and EDS analysis (Figures 1 and 2). In the study, rutile TiO_2 NFs were obtained without any additional post-heat treatment or annealing process, which is usually required by most of the fabrication techniques such as electrospinning and anodization, and thus, this method offers the advantage of being cost-effective.[29] In addition, the contact angle and XRD results showed that this surface modification treatment improved the surface wettability of the substrate and changed the surface crystal structure (Figure 2). It has been reported that an increase in the surface wettability of the scaffold leads to improved cell attachment and spreading.[35] Taken together, we expect that these as-grown nanofibrous surface structures will be of biological interest due to the fact that these nanostructures present a topography that has structural similarity to natural ECM[18] and exhibits improved surface wettability, based on the contact angle measurement analysis.

Cell adhesion is the first response when cells come into contact with a material.[7] It has been reported that cell adhesion is vital in the regulation of subsequent cellular behaviors, such as proliferation, differentiation, and mineralization, as well as gene expression.[5,22] Consequently, ADSCs were cultured on the nanofibrous surface substrates and their initial cell adhesion relative to that of the control substrate after 1, 3, 7, and 14 days of incubation was observed via FESEM as shown in Figure 3. Our results indicate that the TiO_2 nanofibrous surface substrate was favored for initial adhesion of ADSCs. It was seen that by day 14, ADSCs cultured on the nanofibrous surfaces had extended their filopodia

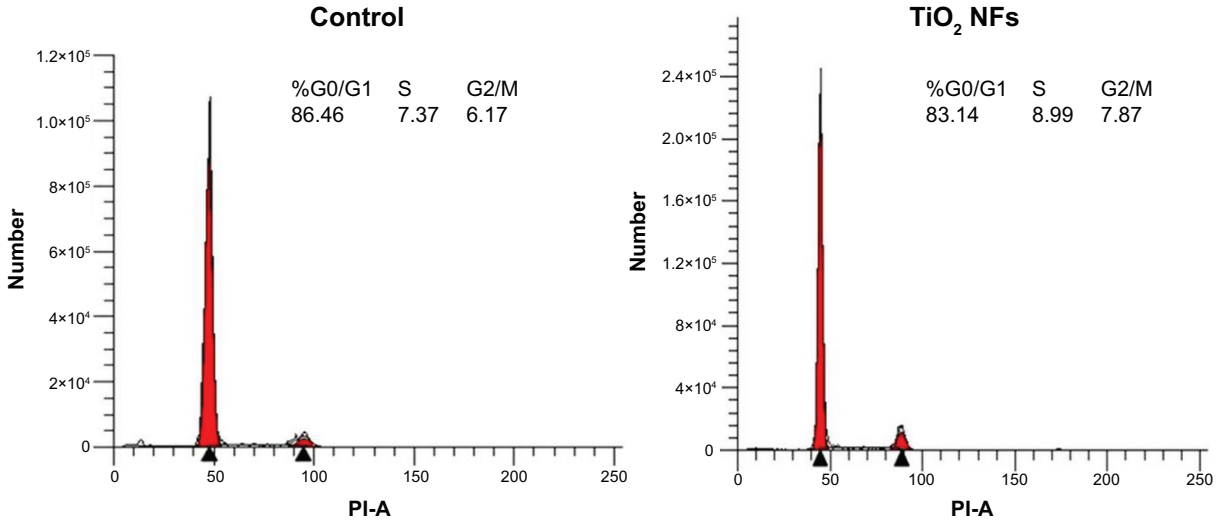

Figure 5 Representative DNA histogram of ADSCs cultured on control Ti-6Al-4V surfaces and TiO_2 nanofibrous surfaces.
Note: The percentages of cells residing in the G0/G1 phase, S phase, and G2/M phase are shown in the histograms.
Abbreviations: ADSCs, adipose-derived stem cells; NFs, nanofibers; PI-A, propidium iodide-area.

Table 2 Percentage of cells at various cell cycle phases and their corresponding PI

Group	Cell cycle phase			
	G0/G1 (%)	S (%)	G2/M (%)	PI (%)
Control	86.53±0.003	7.66±0.003	5.81±0.006	13.47±0.328
TiO_2 NFs	83.02±0.006*	9.27±0.002*	7.68±0.009*	16.95±0.651*

Notes: Data are presented as mean ± standard deviation. Statistical significance was assessed relative to the control sample (*$P<0.05$).
Abbreviations: NF, nanofiber; PI, proliferation index.

and contacted the adjoining cells to form an intercellular network, indicating good quality cell adhesion. A likely explanation for this observation is that larger surface areas are provided by the as-grown nanofibrous surfaces, offering more attachment sites for the cells to contact and adhere to. In addition, their irregular nanofibrillar structures provide cues for the cells to anchor to and thus contribute to the lock-in cell configuration.[36] As evidenced in Figure 3, it can also be clearly seen that the as-grown TiO_2 NFs were presented on the substrate surface until day 14, up to which the in vitro cell study was performed. This observation implies that the as-grown NFs were chemically stable since they were not degraded by the culture medium employed in the study. Further investigations concerning the stability and strength of these as-grown NFs in vivo would be valuable.

Apart from good initial cell adhesion, an ideal scaffold should also possess the potential to actively stimulate cell proliferation. Cell proliferation is the process whereby cells reproduce themselves as a result of cell growth and division. In this study, we assessed the proliferation of ADSCs on both the surfaces by measuring their cell number using the AlamarBlue assay after 2 weeks of cell incubation. Our results (as revealed in Figure 4) showed that the as-grown TiO_2 nanofibrous surfaces were beneficial for ADSCs proliferation, with the number of cells significantly higher than that on the plain substrate at all time intervals. In the study by Park et al the authors reported that TiO_2 nanotubes with a diameter ranging 30–50 nm resulted in better cell growth due to integrin clustering and the formation of adhesion complexes.[37] In this study, the diameter of the as-produced TiO_2 NFs was around 50 nm. We speculated that the range of diameter obtained in the present study could be beneficial to the integrin clustering, promoting initial cell adhesion and spreading using the fiber features as anchoring points, and thus leading to an increase in cell proliferation on the nanofibrous surfaces relative to the control surfaces. The results obtained for cell proliferation as presented in Figure 4 are in accordance with the observation of cell adhesion as revealed in Figure 3. It is important that the proliferative ADSCs do not precede aneuploidy stage that attain the malignant

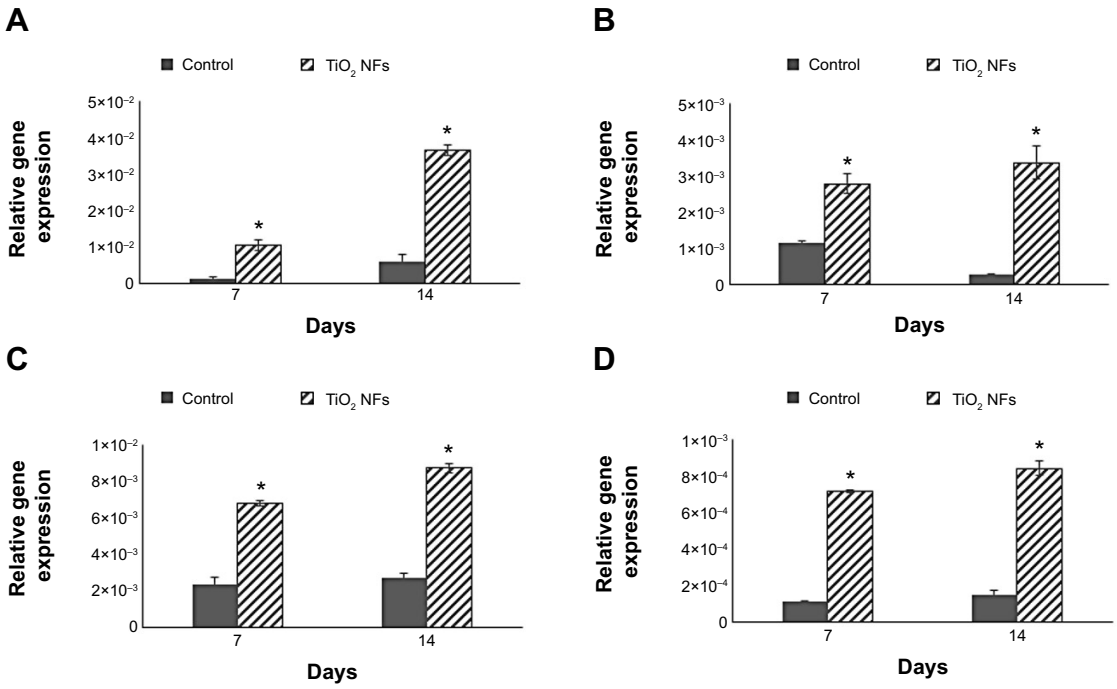

Figure 6 Relative expression of cell cycle–regulated genes: (**A**) *CyclinD1*, (**B**) *pRb*, (**C**) *GADD45*, and (**D**) *p53*, by ADSCs cultured on both the control and TiO_2 nanofibrous surfaces for 7 days and 14 days.
Note: Statistical significance was assessed relative to the control sample for each time interval (*$P<0.05$).
Abbreviations: ADSCs, adipose-derived stem cells; NFs, nanofibers.

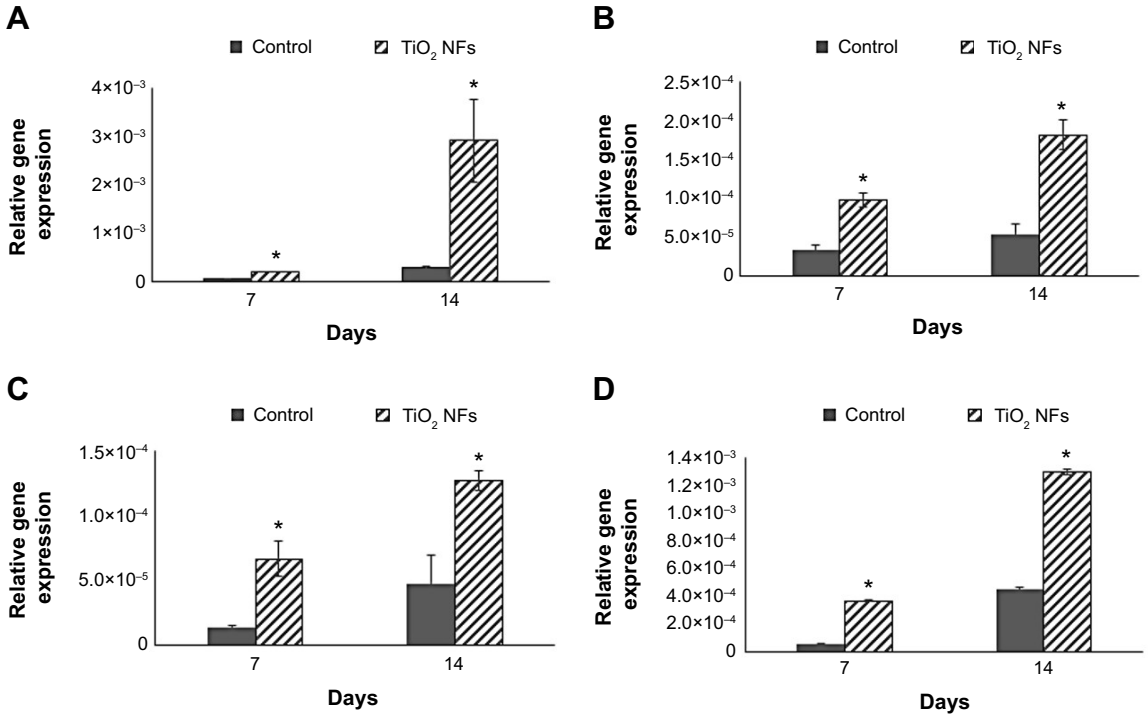

Figure 7 Relative expression of stemness marker genes: (**A**) *Nanog3*, (**B**) *Rex-1*, (**C**) *Sox-2*, and (**D**) *Nestin*, by ADSCs cultured on both the control and TiO_2 nanofibrous surfaces for 7 days and 14 days.
Note: Statistical significance was assessed relative to the control sample for each time interval (*$P<0.05$).
Abbreviations: ADSCs, adipose-derived stem cells; NFs, nanofibers.

phenotype.[38] To verify this issue, cell cycle analysis was performed to determine the DNA content and the percentage of cells during proliferation at various phases. Our results as shown in Figure 5 and Table 2 further corroborate that TiO_2 nanofibrous surfaces possess greater proliferation ability of ADSCs while maintaining the normal diploid state of the cells in comparison to the untreated control surfaces.

The relationship between the substrate topography and ADSCs proliferation was further quantified at the molecular level by comparing the expression of cell cycle–regulated genes in both the sample surfaces. The cell cycle–regulated genes of interest in this study were CyclinD1, pRb, GADD45, and p53. As exemplified in Figure 6, the expressions of all the cell cycle–regulated genes were significantly higher on the nanofibrous surfaces than on the corresponding untreated control surfaces. CyclinD1 is known to be one of the cyclin protein family that is involved in the regulation of cell cycle progression through activation of cyclin-dependent kinase (Cdk) enzymes.[38] In the normal cell cycle, the synthesis of cyclinD1 is initiated during the G1 phase. They promote the G1 to S phase transition by forming an active complex with Cdk and cause the phosphorylation of the retinoblastoma tumor suppressor protein (pRb) to activate the E2F transcriptional system.[38] Therefore, the expression of cyclinD1 is regulated positively by pRb. Our results support this view that TiO_2 nanofibrous surfaces upregulate cyclinD1 expression, which is followed by a subsequent increase in pRb expression. However, this phenomenon was not observed on the control surfaces, implying that nanofibrous surfaces may have an effect on facilitating the S phase entry. These findings are further supported by the significant reduction in the number of cells in the G0/G1 phase of the cell cycle as shown in Table 2. The number of cells in the G0/G1 phase of the cell cycle decreased significantly from 86.53%±0.003% in control surfaces to 83.02%±0.006% in the TiO_2 nanofibrous surfaces ($P<0.05$), indicating accelerated entry into the S phase.[39]

Further, we were interested to investigate whether the proliferating cells are undergoing normal cell proliferation process since uncontrolled proliferation has been reported as a hallmark of cancer.[40] Herein, we compare the gene expression of two tumor suppressor genes, that are pRb and p53, on both the sample surfaces. Our data in Figure 6 show that TiO_2 nanofibrous surfaces displayed significant upregulation of pRb and p53 expression in a time-dependent manner, which is in line with the trend of the aforementioned cell proliferation results, suggesting that TiO_2 NFs can promote cell proliferation while keeping the process under control. These observations are further supported by the significant

upregulation of GADD45 expression on the nanofibrous surfaces compared to their control counterparts. GADD45 is one of the growth arrest and DNA-damage–inducible genes (GADD) that plays a pivotal role in cellular genotoxic and nongenotoxic stress responses, acting as stress sensor and tumor suppressors.[41] Studies have shown that cells exhibit uncontrolled proliferation when GADD45 is repressed.[42] Altogether, the results presented here show that TiO_2 nanofibrous surface structures could account for their morphogenic effect in triggering cell proliferation and regulating normal cell cycle progression.

While the role of substrate nanotopography has been shown in modulating the regulation of cell proliferation, it is also crucial to study the impact of this factor on retaining the stemness of ADSCs. Sox-2, Rex-1, Nanog3, and Nestin are regarded as the stemness markers in this study. Sox-2 is a transcription factor that is essential for preserving self-renewal and pluripotency of undifferentiated embryonic stem cells.[43] Same as Sox-2, Nanog3 is also a marker for embryonic stem cell pluripotency and self-renewal and its role in regulating the expression of Rex-1 by binding to its promoter has been reported in some studies.[43,44] As one of the known pluripotency transcription factors, Rex-1 is usually found in undifferentiated embryonic stem cells and its expression is severely downregulated upon stem cell differentiation.[43,45] Nestin is known as a neural stem cell marker that is often expressed in its early stage or progenitor cells.[46] The presence of all these markers has been commonly found in embryonic stem cells, and thus, their expression is important to mark their pluripotency and self-renewal capabilities.[12,43] Our qRT-PCR results as revealed in Figure 7 show that substrate nanotopography tends to regulate the stemness of ADSCs. It was observed that the expression level of these stemness markers on the TiO_2 nanofibrous surfaces was significantly higher relative to the control surfaces at all time intervals, supporting that TiO_2 nanofibrous surfaces are preferential for preserving ADSCs stemness. Moreover, given the enhanced expression of Nestin on ADSCs cultured on nanofibrous surfaces, these results might implicate the possibility that these nanofibrous surfaces can transdifferentiate ADSCs into cells of nonmesenchymal lineages such as neurocytes upon the stimuli caused by the structural nanocues on the substrate topography. Combining the results presented above, we confirmed our hypothesis that the TiO_2 nanofibrous surface fabricated by using thermal oxidation in this study could promote better cell adhesion and proliferation while simultaneously maintaining the stemness of ADSCs. The enhanced stemness maintenance capability is presumably due to the stress induced during cell adhesion to the underlying nanofibrous surface structures.[47] The nanotopographical cues that presented on the TiO_2 nanofibrous surfaces are reported to resemble the structural features of the ECM that provide physical anchorages to the adhesive molecules such as integrins on the cell membrane.[48] The forces generated during cell adhesion are transmitted to the nucleus through the cytoskeleton network to activate a downstream mechanotransduction pathway within the cells.[47] The resulting cascade reactions modulate gene expression and signal transduction, which are responsible for the upregulation of cell stemness.[49,50] However, the underlying mechanism of the cascade reaction in regulating the cell stemness is not entirely understood and remains to be elucidated.

Titanium and its alloys have been well-explored as biomaterials in various biomedical applications, especially in orthopedic applications such as bone plate, dental implants, knee joint, and bone void filler due to their favorable mechanical properties, excellent biocompatibility, and very good corrosion resistance.[47] However, they do not promote osteointegration due to their low bioactivity.[18] In our work presented here, we have demonstrated the utility of TiO_2 NFs by thermal oxidation in enhancing the bioactivity of Ti-6Al-4V while preserving their advantages as mentioned above. Thus, we foresee that these TiO_2 nanofibrous surface structures can be beneficial for the potential application of bone tissue engineering and regeneration as they are able to maintain the stemness and self-renewal capability of ADSCs, which will significantly shorten the healing time. This will be favorable in any clinical situation as it can reduce medical costs and speed up recovery of the patients.

Although this study demonstrates the role of substrate nanotopography in regulating cell proliferation while maintaining the pluripotency state of stem cells, there is another remaining issue that should be addressed in future. Considering the two important goals in stem cell research involving biomaterials as mentioned earlier, the exact role of substrate topography in directing the desired differentiation without the use of biological stimuli such as inducing media and growth factors remains to be determined.

Conclusion

In this study, in situ TiO_2 NFs were fabricated onto the surface of Ti-6Al-4V substrate via a thermal oxidation process, which was then characterized by several techniques such as FESEM, EDS, XRD, and contact angle measurement; the results revealed that TiO_2 NFs possess greater degree of crystallinity and surface wettability. In vitro tests using

ADSCs confirmed that these as-grown nanofibrous surface structures promote cell adhesion and proliferation while maintaining the stemness of ADSCs. These findings present promising potential for applications of TiO_2 nanofibrous surface structures in the field of bone tissue engineering as well as for regenerative therapies.

Acknowledgments

The authors gratefully acknowledge support by a High Impact Research Grant (UM.C/HIR/MOHE/ENG/44) funded by the Higher Education of Malaysia and Postgraduate Research Fund (PV 102/2012A) from the University of Malaya.

Disclosure

The authors report no conflicts of interest in this work.

References

1. Wu KC, Tseng CL, Wu CC, et al. Nanotechnology in the regulation of stem cell behavior. *Sci Technol Adv Mater.* 2013;14(5):054401.
2. Tan AW, Pingguan-Murphy B, Ahmad R, Akbar SA. Review of titania nanotubes: fabrication and cellular response. *Ceram Int.* 2012;38(6): 4421–4435.
3. Zhang D, Kilian KA. The effect of mesenchymal stem cell shape on the maintenance of multipotency. *Biomaterials.* 2013;34(16):3962–3969.
4. Logan N, Brett P. The control of mesenchymal stromal cell osteogenic differentiation through modified surfaces. *Stem Cells Int.* 2013;2013: 361637.
5. Lai M, Cai KY, Hu Y, Yang XF, Liu Q. Regulation of the behaviors of mesenchymal stem cells by surface nanostructured titanium. *Colloid Surf B Biointerfaces.* 2012;97:211–220.
6. Kaitainen S, Mähönen AJ, Lappalainen R, Kröger H, Lammi MJ, Qu CJ. TiO_2 coating promotes human mesenchymal stem cell proliferation without the loss of their capacity for chondrogenic differentiation. *Biofabrication.* 2013;5(2):025009.
7. Liu Q, Cen L, Yin S, et al. A comparative study of proliferation and osteogenic differentiation of adipose-derived stem cells on akermanite and beta-TCP ceramics. *Biomaterials.* 2008;29(36):4792–4799.
8. Motemani Y, Greulich C, Khare C, et al. Adherence of human mesenchymal stem cells on Ti and TiO_2 nano-columnar surfaces fabricated by glancing angle sputter deposition. *Appl Surf Sci.* 2014;292:626–631.
9. Lim JY, Loiselle AE, Lee JS, Zhang Y, Salvi JD, Donahue HJ. Optimizing the osteogenic potential of adult stem cells for skeletal regeneration. *J Orthop Res.* 2011;29(11):1627–1633.
10. Hui C, Safwani W, Chin S, et al. Human serum promotes the proliferation but not the stemness genes expression of human adipose-derived stem cells. *Biotechnol Bioproc Eng.* 2012;17(6):1306–1313.
11. Schreml S, Babilas P, Fruth S, et al. Harvesting human adipose tissue-derived adult stem cells: resection versus liposuction. *Cytotherapy.* 2009;11(7):947–957.
12. Yu J, Tu YK, Tang YB, Cheng NC. Stemness and transdifferentiation of adipose-derived stem cells using L-ascorbic acid 2-phosphate-induced cell sheet formation. *Biomaterials.* 2014;35(11):3516–3526.
13. Guilak F, Lott KE, Awad HA, et al. Clonal analysis of the differentiation potential of human adipose-derived adult stem cells. *J Cell Physiol.* 2006;206(1):229–237.
14. Zuk PA, Zhu M, Mizuno H, et al. Multilineage cells from human adipose tissue: implications for cell-based therapies. *Tissue Eng.* 2001;7(2): 211–228.
15. McNamara LE, McMurray RJ, Biggs MJ, Kantawong F, Oreffo RO, Dalby MJ. Nanotopographical control of stem cell differentiation. *J Tissue Eng.* 2010:120623.
16. Oh S, Brammer KS, Li YS, et al. Stem cell fate dictated solely by altered nanotube dimension. *Proc Natl Acad Sci U S A.* 2009;106(7): 2130–2135.
17. Ravichandran R, Ng CC, Liao S, et al. Biomimetic surface modification of titanium surfaces for early cell capture by advanced electrospinning. *Biomed Mater.* 2012;7(1):015001.
18. Tan A, Pingguan-Murphy B, Ahmad R, Akbar S. Advances in fabrication of TiO_2 nanofiber/nanowire arrays toward the cellular response in biomedical implantations: a review. *J Mater Sci.* 2013;48(24): 8337–8353.
19. Bauer S, Park J, von der Mark K, Schmuki P. Improved attachment of mesenchymal stem cells on super-hydrophobic TiO_2 nanotubes. *Acta Biomater.* 2008;4(5):1576–1582.
20. Chen XY, Cai KY, Lai M, Zhao L, Tang LL. Mesenchymal stem cells differentiation on hierarchically micro/nano-structured titanium substrates. *Adv Eng Mater.* 2012;14(5):B216–B223.
21. Brammer KS, Choi C, Frandsen CJ, Oh S, Jin S. Hydrophobic nanopillars initiate mesenchymal stem cell aggregation and osteo-differentiation. *Acta Biomater.* 2011;7(2):683–690.
22. Hu Y, Cai KY, Luo Z, et al. Regulation of the differentiation of mesenchymal stem cells in vitro and osteogenesis in vivo by microenvironmental modification of titanium alloy surfaces. *Biomaterials.* 2012; 33(13):3515–3528.
23. Nava MM, Raimondi MT, Pietrabissa R. Controlling self-renewal and differentiation of stemcells via mechanical cues. *J Biomed Biotechnol.* 2012;2012:797410.
24. Dalby MJ, Gadegaard N, Tare R, et al. The control of human mesenchymal cell differentiation using nanoscale symmetry and disorder. *Nat Mater.* 2007;6(12):997–1003.
25. Hou YH, Cai KY, Li JH, et al. Effects of titanium nanoparticles on adhesion, migration, proliferation, and differentiation of mesenchymal stem cells. *Int J Nanomedicine.* 2013;8:3619–3630.
26. Pittrof A, Park J, Bauer S, Schmuki P. ECM spreading behaviour on micropatterned TiO_2 nanotube surfaces. *Acta Biomater.* 2012;8(7): 2639–2647.
27. Frandsen CJ, Brammer KS, Noh K, Johnston G, Jin S. Tantalum coating on TiO_2 nanotubes induces superior rate of matrix mineralization and osteofunctionality in human osteoblasts. *Mater Sci Eng C Mater Biol Appl.* 2014;37:332–341.
28. Tan AW, Dalilottojari A, Pingguan-Murphy B, Ahmad R, Akbar S. In vitro chondrocyte interactions with TiO_2 nanofibers grown on Ti6-Al-4V substrate by oxidation. *Ceram Int.* 2014;40(6):8301–8304.
29. Wang XD, Shi J. Evolution of titanium dioxide one-dimensional nanostructures from surface-reaction-limited pulsed chemical vapor deposition. *J Mater Res.* 2013;28(3):270–279.
30. Lee H, Dregia S, Akbar S, Alhoshan M. Growth of 1-D TiO_2 nanowires on Ti and Ti alloys by oxidation. *J Nanomaterials.* 2010;2010: 503186.
31. Dinan B, Gallego-Perez D, Lee H, Hansford D, Akbar SA. Thermally grown TiO_2 nanowires to improve cell growth and proliferation on titanium based materials. *Ceram Int.* 2013;39(5):5949–5954.
32. Patterson AL. The Scherrer formula for x-ray particle size determination. *Phys Rev.* 1939;56(10):978–982.
33. Blanco R, Rengifo CE, Cedeño M, Frómeta M, Rengifo E. Flow cytometric measurement of aneuploid DNA content correlates with high S-phase fraction and poor prognosis in patients with non-small-cell lung cancer. *ISRN Biomarkers.* 2013;2013:354123.
34. Li D, Lei Y, Deng J, et al. Human but not laboratory Borna disease virus inhibits proliferation and induces apoptosis in human oligodendrocytes in vitro. *PLoS One.* 2013;8(6):e66623.
35. Lord MS, Foss M, Besenbacher F. Influence of nanoscale surface topography on protein adsorption and cellular response. *Nano Today.* 2010;5(1):66–78.
36. Oh S, Jin S. Titanium oxide nanotubes with controlled morphology for enhanced bone growth. *Mater Sci Eng C.* 2006;26(8):1301–1306.
37. Park J, Bauer S, von der Mark K, Schmuki P. Nanosize and vitality: TiO_2 nanotube diameter directs cell fate. *Nano Lett.* 2007;7(6):1686–1691.

38. Fatimah SS, Tan GC, Chua KH, Tan AE, Hayati AR. Effects of epidermal growth factor on the proliferation and cell cycle regulation of cultured human amnion epithelial cells. *J Biosci Bioeng.* 2012;114(2):220–227.
39. Taylor BK, Stoops TD, Everett AD. Protein phosphatase inhibitors arrest cell cycle and reduce branching morphogenesis in fetal rat lung cultures. *Am J Physiol Lung Cell Mol Physiol.* 2000;278(5):L1062–L1070.
40. Chen X, Lowe M, Herliczek T, et al. Protection of normal proliferating cells against chemotherapy by staurosporine-mediated, selective, and reversible G(1) arrest. *J Natl Cancer Inst.* 2000;92(24):1999–2008.
41. Tamura RE, de Vasconcellos JF, Sarkar D, Libermann TA, Fisher PB, Zerbini LF. GADD45 proteins: central players in tumorigenesis. *Curr Mol Med.* 2012;12(5):634–651.
42. Cheng D, Zhao L, Zhang L, et al. p53 controls hepatitis C virus nonstructural protein 5A-mediated downregulation of GADD45α expression via the NF-κB and PI3KAkt pathways. *J Gen Virol.* 2013;94(Pt 2):326–335.
43. Fatimah SS, Tan GC, Chua K, Fariha MM, Tan AE, Hayati AR. Stemness and angiogenic gene expression changes of serial-passage human amnion mesenchymal cells. *Microvasc Res.* 2013;86:21–29.
44. Zinger O, Zhao G, Schwartz Z, et al. Differential regulation of osteoblasts by substrate microstructural features. *Biomaterials.* 2005;26(14):1837–1847.
45. Shi W, Wang H, Pan G, Geng Y, Guo Y, Pei D. Regulation of the pluripotency marker Rex-1 by Nanog and Sox2. *J Biol Chem.* 2006;281(33):23319–23325.
46. Dahlstrand J, Lardelli M, Lendahl U. Nestin mRNA expression correlates with the central nervous system progenitor cell state in many, but not all, regions of developing central nervous system. *Brain Res Dev Brain Res.* 1995;84(1):109–129.
47. Brammer KS, Frandsen CJ, Jin S. TiO_2 nanotubes for bone regeneration. *Trends Biotechnol.* 2012;30(6):315–322.
48. Lee MR, Kwon KW, Jung H, et al. Direct differentiation of human embryonic stem cells into selective neurons on nanoscale ridge/groove pattern arrays. *Biomaterials.* 2010;31(15):4360–4366.
49. Lü D, Luo C, Zhang C, Li Z, Long M. Differential regulation of morphology and stemness of mouse embryonic stem cells by substrate stiffness and topography. *Biomaterials.* 2014;35(13):3945–3955.
50. Hashemi SM, Soudi S, Shabani I, Naderi M, Soleimani M. The promotion of stemness and pluripotency following feeder-free culture of embryonic stem cells on collagen-grafted 3-dimensional nanofibrous scaffold. *Biomaterials.* 2011;32(30):7363–7374.